

# Resolving Biodegradation Patterns of Persistent Saturated Hydrocarbons in Weathered Oil Samples from the *Deepwater Horizon* Disaster

Jonas Gros,<sup>†,‡</sup> Christopher M. Reddy,<sup>§</sup> Christoph Aeppli,<sup>§,||</sup> Robert K. Nelson,<sup>§</sup> Catherine A. Carmichael,<sup>§</sup> and J. Samuel Arey<sup>\*,†,‡</sup>

<sup>†</sup>Environmental Chemistry Modeling Laboratory, GR C2 544, Swiss Federal Institute of Technology at Lausanne (EPFL), Station 2, CH-1015 Lausanne, Switzerland

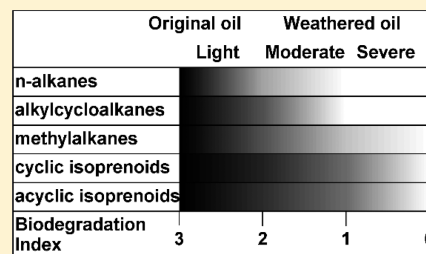
<sup>‡</sup>Department of Environmental Chemistry, Swiss Federal Institute of Aquatic Science and Technology (Eawag), Überlandstrasse 133, CH-8600 Dübendorf, Switzerland

<sup>§</sup>Department of Marine Chemistry and Geochemistry, Woods Hole Oceanographic Institution, 266 Woods Hole Road, Woods Hole, Massachusetts 02543, United States

## Supporting Information

**ABSTRACT:** Biodegradation plays a major role in the natural attenuation of oil spills. However, limited information is available about biodegradation of different saturated hydrocarbon classes in surface environments, despite that oils are composed mostly of saturates, due to the limited ability of conventional gas chromatography (GC) to resolve this compound group. We studied eight weathered oil samples collected from four Gulf of Mexico beaches 12–19 months after the *Deepwater Horizon* disaster. Using comprehensive two-dimensional gas chromatography (GC×GC), we successfully separated, identified, and quantified several distinct saturates classes in these samples. We find that saturated hydrocarbons eluting after *n*-C<sub>22</sub> dominate the GC-amenable fraction of these weathered samples.

This compound group represented 8–10%, or 38–68 thousand metric tons, of the oil originally released from Macondo well. Saturates in the *n*-C<sub>22</sub> to *n*-C<sub>29</sub> elution range were found to be partly biodegraded, but to different relative extents, with ease of biodegradation decreasing in the following order: *n*-alkanes > methylalkanes and alkylcyclopentanes+alkylcyclohexanes > cyclic and acyclic isoprenoids. We developed a new quantitative index designed to characterize biodegradation of >*n*-C<sub>22</sub> saturates. These results shed new light onto the environmental fate of these persistent, hydrophobic, and mostly overlooked compounds in the unresolved complex mixtures (UCM) of weathered oils.



## INTRODUCTION

Biodegradation is a major transformation process for petroleum hydrocarbons in both surface and subsurface environments.<sup>1–3</sup> However, it is not uniform, varying in extent, compound specificity, and relative rates for different compounds, depending on environmental conditions.<sup>3,4</sup> Oil residues can persist for years in the environment without exhibiting any significant sign of biodegradation,<sup>5</sup> whereas under other conditions 40% of the oil can be degraded within one month.<sup>2</sup> Additionally, biodegradability depends on oil composition, because different compounds exhibit different susceptibilities to biodegradation.<sup>3,6,7</sup> To understand the spectrum of fates of spilled hydrocarbons, it is therefore essential to account for the rate, extent, and possible cessation of biodegradation in relevant environmental contexts. In this paper, we assess the biodegradation of several classes of saturated hydrocarbons (“saturates”) that are difficult to resolve and that can persist in weathered oils in surface environments.

Saturates often dominate the gas chromatography (GC)-amenable fraction of moderately weathered oils in surface environments,<sup>8–11</sup> typically described as an “unresolved

complex mixture” (UCM) of compounds that are difficult or impossible to separate using conventional GC-based techniques.<sup>12</sup> Early stages of weathering are typified by the loss of light compounds (<15–20 carbons) from the oil mixture through evaporation,<sup>13</sup> as well as loss of two- to four-ring polycyclic aromatic hydrocarbons (PAHs) by evaporation, aqueous dissolution, and photodegradation.<sup>1,7,14,15</sup> The remaining compounds in the weathered oil, which are subject to removal principally by biodegradation,<sup>4,7</sup> are usually mostly saturates.<sup>8–11</sup> This oil fraction includes easily biodegradable *n*-alkanes and more resistant branched and cyclic compounds,<sup>3,16</sup> as well as some highly recalcitrant biomarkers such as hopanes or steranes<sup>17</sup> that biodegrade only under extreme conditions.<sup>18</sup> Indirect photodegradation can also affect saturates,<sup>19–21</sup> although the time frame of this process under relevant environmental conditions remains unclear.

Received: September 25, 2013

Revised: December 11, 2013

Accepted: December 18, 2013

Despite the prominence of saturates in weathered oils,<sup>11</sup> presently available approaches to diagnose biodegradation are centered mostly on PAHs and highly recalcitrant biomarkers.<sup>3,16</sup> Several different biodegradation indices, formulated as compound concentration ratios,<sup>2,22</sup> have been proposed to diagnose biodegradation in weathered oil; however most of these ratios involve PAHs and/or biomarkers (see reference 23 for a compilation). In a recent review, biodegradability rankings for the “>C<sub>15</sub> category” included 10 PAH groups, 7 biomarker groups, and only 2 saturates groups (*n*-alkanes+isoalkanes group and isoprenoids group).<sup>3</sup> These biases partly reflect the wide use of conventional GC, which effectively separates and quantifies PAHs in weathered petroleum mixtures, but which is less effective at separating structural isomers of saturates,<sup>24,25</sup> thus giving rise to the “unresolved” fraction of weathered oil, or UCM.<sup>12</sup>

Compared to PAHs, limited information is available about biodegradation of different saturates classes in surface environments. Both laboratory<sup>26–28</sup> and field<sup>29,30</sup> studies have reported preferential biodegradation of *n*-alkanes versus acyclic isoprenoids and cycloalkanes in surface environments. However most knowledge about hydrocarbons biodegradation comes from subsurface reservoir studies.<sup>3,16,31</sup> In subsurface environments, decreasing susceptibility to biodegradation is observed in the following order: *n*-alkanes > 2-methyl- and 3-methyl-alkanes > alkylcyclohexanes and methylalkylcyclopentanes > acyclic isoprenoids.<sup>32</sup> It remains unclear whether these trends are transferable to surface environments, where oil mixtures experience very different conditions and residence times compared to subsurface environments.

Studies on oil toxicity have largely focused on aromatic components that have important acute and chronic toxicity.<sup>4,9</sup> However few studies have addressed the toxicity arising from saturates-dominated UCMs.<sup>9</sup> Narcotic-based toxicity of UCMs<sup>10,33</sup> cannot be explained by resolved compounds only,<sup>34</sup> and Scarlett et al. demonstrated toxicity of the aliphatic fraction of UCMs that had been previously regarded as nontoxic.<sup>35</sup>

How can we gain better insight into the composition and behavior of saturates-dominated UCMs in the environment? Comprehensive two-dimensional gas chromatography (GC×GC) provides well-resolved compositional information for weathered oil UCMs, including separation of saturates.<sup>15,36–38</sup> This technique uses two serially joined columns to separate thousands of compounds in complex mixtures of petroleum hydrocarbons. GC×GC produces a distinct elution pattern for each hydrocarbon compound class, providing an elementary means to differentiate compound classes, as well as individual compounds within a class. This enables detailed knowledge about the state of biodegradation of oil. For example, Wardlaw et al. used GC×GC coupled to a flame ionization detector (FID) to study the compositional evolution of oil that was biodegraded during subsurface ascent from a reservoir to the sea floor.<sup>6</sup> More recently, Mao et al. drew hydrocarbon-group windows on GC×GC-FID chromatograms to study accelerated hydrocarbons biodegradation occurring in aerobic “biopiles”.<sup>39</sup> Mao et al. successfully separated different saturates classes, observing the following decreasing biodegradability preference: *n*-alkanes > branched alkanes > cyclic alkanes.

In the present study, we sought to expand information available about the biodegradation of saturated hydrocarbons occurring in the UCMs of weathered oils in surface

environments. We used beached oil samples from the *Deepwater Horizon* oil release that exhibited typical signs of moderate saturates biodegradation. The *Deepwater Horizon* disaster was likely the largest accidental marine oil release in history<sup>40</sup> and emitted 470–690 thousands of metric tons of oil into the marine environment.<sup>41,42</sup> This included 62%<sup>11</sup> to 74%,<sup>41</sup> or 291–511 thousand metric tons, of saturated oil hydrocarbons. Despite massive cleanup and countermeasure efforts, oil-soaked sand patties continue to wash ashore<sup>11</sup> more than 3 years after the release. We studied saturates biodegradation in beached oil samples that were taken at four different locations at several time points 12–19 months after the release event. Relative to the original Macondo well (MW) oil, these samples had partly or totally lost the most volatile (<*n*-C<sub>18</sub>) and soluble compounds, providing an excellent example in which traditional GC-based techniques did not resolve meaningful compositional differences in the UCM. Using GC×GC, we observed systematic patterns in the ordering and relative extent of biodegradation among different classes of saturates compounds in these samples. The presented data improve our understanding of the compositional changes in the UCM arising from biodegradation in surface environments. This could inform future assessments of the toxicity and environmental impact of the persistent and poorly understood hydrocarbon UCM fraction of weathered oil.

## MATERIALS AND METHODS

**Sample Collection.** Oil-soaked sand patties were collected from April to November 2011, 12–19 months after the beginning of the *Deepwater Horizon* oil release (Figure 1).

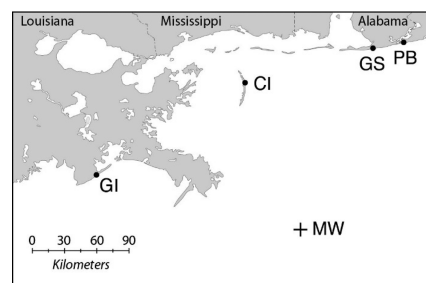


**Figure 1.** Sampling locations. The cross (+) indicates the position of the Macondo well (MW). Samples B60 and B92 were collected at Perdido Beach (PB). B10, B61, B93 and B94 were collected at Gulf Shores (GS). B48 and B86 were collected at Chandeleur Islands (CI) and Grand Isle (GI), respectively.<sup>11</sup>

Samples were composed of either a single patty or a composite of several patties collected within a few meters of each other. They were obtained from sites as far away as 200 km from the MW site, including Perdido Beach, FL (PB), Gulf Shores, AL (GS), Chandeleur Islands, LA (CI), and Grand Isle, LA (GI). Eight samples in total were studied: B60; B92, B10, B61, and B93; B94 and B48; and B86, at PB, GS, CI, and GI, respectively. This labeling scheme was used by Aeppli et al., who confirmed that all of these samples were MW oil residues using hopane and sterane biomarkers.<sup>11</sup> Detailed information about the weathered samples is available in the Supporting Information (Section S-1). Original, neat MW oil has been fully characterized elsewhere.<sup>41</sup> Samples were taken from both “dry” locations, high above the usual shoreline (B48, B86, B92), and “wet” locations, from within the surf zone (<0.5 m depth) or intertidal zone (B10, B60, B61, B93, B94). Detailed sampling

environment descriptions are given for each sample (SI Table S-1).

**Sample Extraction.** Approximately 50 g of each sample was Soxhlet extracted in dichloromethane/methanol (90/10) for 24 h. For sub-samples, the solvent was removed via rotary evaporation, and a total extractable mass was obtained. Extracts dissolved in dichloromethane/methanol were stored at room temperature until analysis.

**Chemicals.** Standards included normal alkanes, methylalkanes, farnesane, norpristane, pristane, and phytane that were obtained from Sigma-Aldrich. Alkylcyclohexanes, (4,8-dimethylnonyl)benzene, (4,8-dimethylnonyl)cyclohexane, 1,3-dimethyl-2-(3,7-dimethyloctyl)benzene, and 1,3-dimethyl-2-(3,7-dimethyloctyl)cyclohexane were bought from Chiron (Norway). Linear alkylbenzenes and PAHs were supplied by Sigma-Aldrich and Alltech. C<sub>30</sub> 17 $\alpha$ (H),21 $\beta$ (H)-hopane and other biomarker standards were obtained from Chiron and the National Institute of Standards and Technology. Professor Roger Summons (MIT) kindly provided us alkylcyclopentanes synthesized in his laboratory.

**GC-FID.** GC-FID analysis of sample extracts was performed on a Hewlett-103 Packard 5890 Series II GC. Samples were injected splitless and separated on a Restek Rtx-1 capillary column (30 m, 0.25 mm inner diameter (I.D.), 0.25  $\mu$ m film thickness) with 5 mL min<sup>-1</sup> H<sub>2</sub> as the carrier gas. The temperature program was 7 min at 35 °C, followed by ramp to 315 °C at 6 °C min<sup>-1</sup> and then to 320 °C at 20 °C min<sup>-1</sup> (held 15 min).

**GC×GC-FID.** Sample extracts were injected splitless on a GC×GC-FID (Leco, St. Joseph, MI) having an Rtx-1 first-dimension column (60 m, 0.25 mm I.D., 0.25  $\mu$ m film) and an SGE BPX-50 second-dimension column (1.25 m, 0.10 mm I.D., 0.10  $\mu$ m film). The carrier gas was H<sub>2</sub> at a constant flow rate of 0.95 mL min<sup>-1</sup>. The inlet temperature was held at 300 °C. The first oven was programmed as follows: hold at 40 °C for 10 min, ramp from 40 to 340 °C at 1.00 °C min<sup>-1</sup> (held 5 min). The second oven was programmed as follows: hold at 45 °C for 10 min, ramp from 45 to 345 °C at 1.00 °C min<sup>-1</sup> (held 5 min). The modulation period was 15 s. The modulation was carried out using a two-stage modulator, cooled with liquid nitrogen.

Using a series of calibration solutions of standards, we determined that the relative response factors of petroleum hydrocarbons in our samples were all near unity (root mean squared deviation of  $\sim$ 10% for saturates in the *n*-C<sub>25</sub> region), for both GC-FID and GC×GC-FID analysis. This implies that total FID signal recorded is proportional to mass present in the samples, which allowed quantification of aggregated compound groups as well as comparisons of mass changes in the entire saturate elution region between different GC×GC chromatograms. To aid in the identification and confirmation of some compounds, samples were also analyzed by GC×GC-TOF-MS, as described in SI Section S-2.

**Data Analysis of GC×GC-FID Chromatograms.** Several operations were performed on the GC×GC-FID data (except where stated otherwise, "GC×GC" refers to GC×GC-FID). First, the baseline was corrected<sup>43,44</sup> and the chromatograms were normalized.<sup>23</sup> Second, retention times were aligned using a recently developed alignment algorithm to allow pixel-by-pixel comparisons between chromatograms,<sup>45</sup> and signal cutoff was defined in order to remove poorly resolved background signal. These tasks were conducted using a combination of prepackaged algorithms and elementary Matlab opera-

tions.<sup>43–45</sup> The techniques are relatively straightforward to apply, and the different steps are described in detail below. Applied Matlab protocols are freely available on request from the authors.

Although GC×GC separates petroleum hydrocarbons more effectively than GC, some areas of the GC×GC chromatogram exhibit a locally elevated baseline, indicative of material that remains unresolved (Figure 2). This occurs especially in the

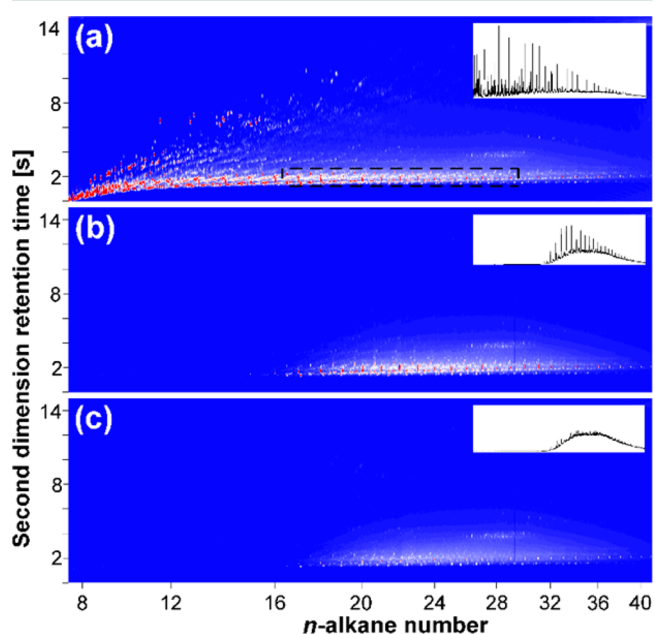


**Figure 2.** GC×GC chromatograms of (a) original MW oil, (b) weathered sample B86, and (c) B92. The black rectangle shows the subregion that was studied in detail. This area contains most of the resolved compound mass of the weathered sample chromatograms (72% for B86 and 59% for B92). Insets: corresponding GC-FID chromatograms (*n*-C<sub>8</sub> to *n*-C<sub>41</sub>) are displayed for comparison.

saturates region of GC×GC chromatograms (Figure 3); hence the choice of baseline treatment may affect quantification of the saturated hydrocarbons. Two different baseline correction methods were applied, reflecting different aims: the method of Reichenbach et al.,<sup>43</sup> in which the baseline is defined conservatively using a white-noise criterion; and the polynomial-fitting baseline estimation code of Eilers.<sup>44</sup> The method of Reichenbach et al., which allows depiction of coeluting material in areas of locally elevated signal, was used for visual comparisons between chromatograms and estimates of total resolved+unresolved mass in the studied subregions of the chromatograms. Default parameters were used (five deadband pixels per modulation; filter window size of seven pixels; ratio of 3.5 for the expected value of baseline plus noise to the estimated standard deviation of the noise; one baseline value per modulation). However, for the quantification of individual resolved compounds, Eilers' baseline correction was applied in order to minimize interference from unresolved material. With appropriate parameters, Eilers' method is designed to follow the base of the resolved peaks, whereas Reichenbach's method preserves unresolved signal. For Eilers' method, we chose parameter values of 10<sup>4</sup> for  $\lambda$ , 0.02 for  $p$ , and 2 for  $d$ . We refer to the signal retained after Eilers' baseline correction as the *resolved* signal.

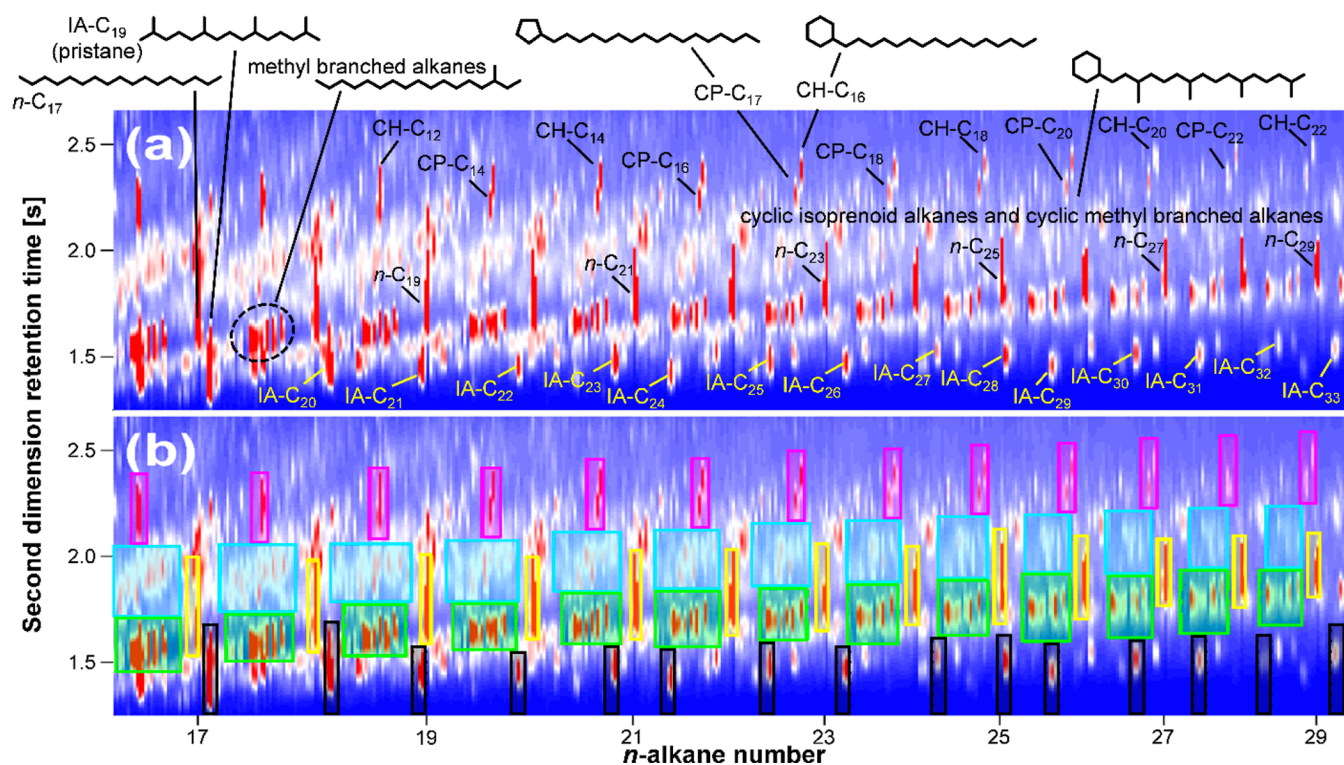


**Figure 3.** (a) Zoom on the GC×GC subregion studied (demarcated in Figure 2a) for the original MW oil chromatogram. (b) Same subregion overlaid with the integration boxes used: acyclic isoprenoids (black rectangle); methylalkanes (green rectangle); *n*-alkanes (yellow rectangle); cyclic isoprenoids (blue rectangle); and acylcyclopentanes and acylcyclohexanes (pink rectangle).

After baseline correction, chromatograms were normalized such that the peak volume of  $C_{30}$   $17\alpha(H),21\beta(H)$ -hopane is the same in all chromatograms. This conserved biomarker is often used to normalize GC×GC chromatograms,<sup>6,14,17,23,36</sup> because it has been found to biodegrade only under extreme conditions. Volumes of the  $C_{30}$   $17\alpha(H),21\beta(H)$ -hopane peaks were computed with the peak-integration algorithm described by Arey et al.<sup>23</sup>

Our analysis focused on the saturates region eluting from *n*-C<sub>17</sub> to *n*-C<sub>29</sub> (Figure 2a), since this represented the dominant GC-amenable fraction of material in collected samples. Retention time reproducibility between chromatograms was improved within this subregion by aligning all the weathered oil chromatograms to the original MW oil chromatogram, using a recently developed algorithm.<sup>45</sup> This method relies on user-selected alignment points that represent identical analytes identified by the user in both the reference (original oil) and target (weathered sample) chromatograms. Twenty-one alignment points were chosen in the subregion studied (SI Figure S-3). Finally, pixels with low remaining signal ( $<10^4$  in FID signal units) were considered to represent noise and poorly resolved background, and these were set to zero. This noise cutoff value corresponded to  $\sim 15\%$  of the apex value of the smallest peak of interest in this study.

For quantification of individual resolved compounds or compound groups, we delineated rectangular borders around each compound or group of compounds. These “boxes” were drawn to include the desired peak or group of peaks, while excluding other compounds or excessive baseline area, in all the chromatograms studied (Figure 3). This approach was considered likely to give consistent results for quantifying signal changes in this very information-dense region of the chromatogram, compared to algorithms<sup>46,47</sup> that attempt to

delineate individual analyte peaks in an automated way. The baseline correction method of Eilers is designed to eliminate low frequency signal arising from poorly resolved material, which enables the estimation of peak volumes by the sum of the pixels included in the boxes. A remaining fraction of  $<15\%$  ( $<5\%$  for *n*-alkanes) in a given box, relative to MW oil, was considered as background and set to zero. Our signal integration procedure is analogous to methods used by Mao and co-workers<sup>39,48</sup> and Frysinger et al.<sup>49</sup>

To estimate the uncertainty of our quantification method, we analyzed our most weathered sample (B93) in triplicate, with 3 GC×GC injections over 3 days. The subsequent numerical treatment was applied separately to each of the 3 chromatograms produced. We obtained standard deviations of 8.8% and 6.1% for quantification of cyclic isoprenoids and acyclic isoprenoids, respectively, relative to  $C_{30}$   $17\alpha(H),21\beta(H)$ -hopane. Other compound classes were mostly degraded in this sample. We thus estimated the overall uncertainties in reported analyte relative abundances to be  $\leq 10\%$ .

## RESULTS AND DISCUSSION

**GC-FID and GC-MS Chromatograms of Weathered Samples.** The GC-FID chromatograms of weathered samples exhibit a poorly separated UCM (insets in Figure 2b,c and SI Figure S-2). This is typical for a GC-FID chromatogram of a weathered crude oil, resulting from ineffective separation of the mixture that remains after the preferential removal of abundant compounds such as *n*-alkanes.<sup>37,50</sup> In response to a suggestion of one reviewer we also briefly investigated whether GC-MS would be effective for the quantification of the compounds studied here. In short, it would be difficult to quantify individual analytes from the resulting mass spectrum data, because individual saturates compounds coelute severely and

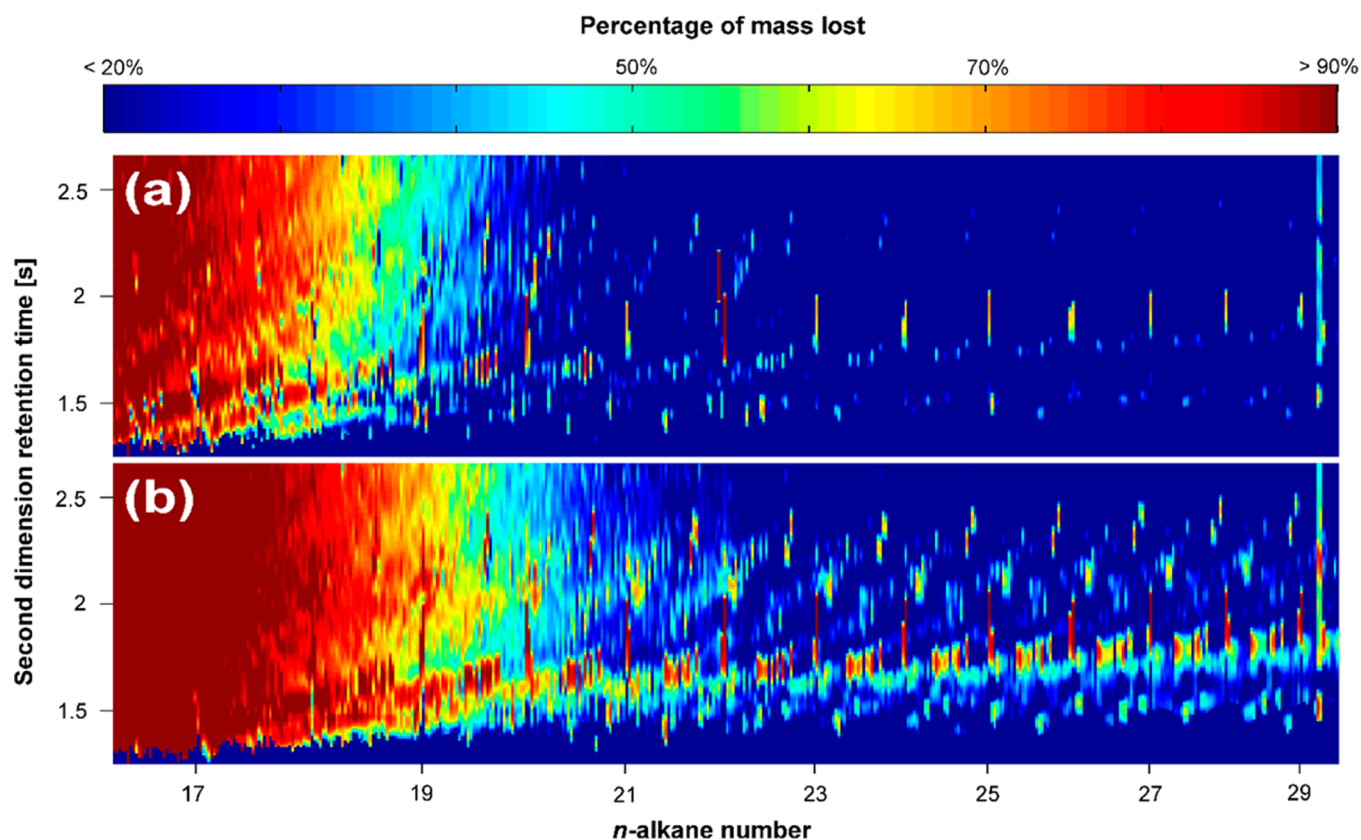


**Figure 4.** Percentage of mass lost, computed pixel by pixel for the GCxGC subregion studied (Figure 2a) relative to original MW oil, for (a) sample B86 and (b) B92. To limit noise in the figure, pixels with signal  $<10^5$  (FID signal units) in MW oil were shaded dark blue. Refer to Figure 3 for the positions of saturates compound classes.

give rise to highly fragmented and very similar spectra (SI Section S-5). Compounds in UCMs, which can arise from samples having different compositions, are estimated to number more than 100 000.<sup>37,51</sup> Beyond a certain extent of biodegradation, all UCMs appear similar (SI Figures S-2c to S-2h); consequently further compositional changes from biodegradation are not discernible.<sup>3</sup> Increased instrument separation capacity is needed to investigate further these apparently compositionally similar UCMs, and to determine whether this similarity is real and whether the biodegraded oil eventually reaches a terminal composition.<sup>37</sup>

**GCxGC Chromatograms of Weathered Samples.** Compared to GC, GCxGC provides improved separation of petroleum-derived UCMs.<sup>15,24</sup> In the GCxGC chromatogram of original MW oil (Figure 2a), *n*-alkanes elute early in the second dimension, forming regularly spaced prominent peaks. Other saturates compounds elute shortly afterward in the second dimension. The biomarkers steranes and hopanes elute between *n*-C<sub>26</sub> and *n*-C<sub>35</sub> in the first dimension and between 3.5 and 5.5 s in the second dimension. PAHs elute earlier than *n*-C<sub>23</sub> in the first dimension and later than 3 s in the second dimension, differentiating them clearly from the saturate region. These elution patterns are typical for petroleum mixtures, as expected from a separation according to volatility in the first dimension and according to polarity in the second dimension.<sup>15,37,52</sup>

GCxGC chromatograms of the weathered samples contained mostly low-volatility saturates. Relative to the neat MW oil, our weathered samples exhibit total loss of two-ring PAHs and >65% loss of three-ring PAHs, as well as losses of

compounds eluting in the *n*-C<sub>8</sub> to *n*-C<sub>18</sub> region (Figure 2). These loss patterns correspond to removal due to aqueous dissolution (which proceeds roughly from the top left corner in the direction of the bottom right corner of the GCxGC chromatograms) and to evaporation (which removes compounds from left to right in the chromatograms).<sup>14,52</sup> These processes have left behind a mixture of which the GC-amenable fraction is mainly saturates having >18 carbons. Due to their low volatilities and low aqueous solubilities,<sup>53</sup> these saturates are not expected to appreciably evaporate or dissolve further. We focused our analysis on the saturates subregion eluting between *n*-C<sub>16</sub> and *n*-C<sub>29</sub> (black rectangle in Figure 2a). This area contains ~60 and ~70% of the resolved GCxGC signal of the weathered samples B92 and B86, respectively. Saturates compounds eluting after *n*-C<sub>22</sub> are most likely acted upon only by biodegradation.<sup>7</sup> The loss patterns of >*n*-C<sub>22</sub> saturates are not consistent with either evaporation or dissolution signatures that are usually observed for lighter compounds,<sup>54,7,13,14</sup> although we note that unusual environmental conditions exceptionally can cause fractionation of >C<sub>22</sub> hydrocarbons.<sup>55</sup> Additionally, saturates are not expected to photodegrade easily, based on their molecular structure<sup>53</sup> and results from photooxidation experiments.<sup>7,56</sup>

The GCxGC subregion depicted in Figure 3 contains five principal saturates classes, annotated on the chromatograms, including *n*-alkanes, methylalkanes, alkylcyclopentanes+alkylcyclohexanes, acyclic isoprenoids, and cyclic isoprenoids. Methylalkanes elute in the order 3-methyl, 2-methyl, 4-methyl, 5-methyl, 6-methyl (decreasing first dimension retention times). Among alkylcycloalkanes, the alkylcyclohexane always

elutes slightly later in the second dimension compared to the alkylcyclopentane structural isomer, and also elutes later in the first dimension for the  $>C_{18}$  carbon isomers. Each compound or compound class was identified with pure standards and using GC×GC-TOF-MS (SI Figure S-7).

To visualize trends of compound mass losses, we applied algebraic operations directly to the chromatographic data and thus constructed pixel-by-pixel percent mass loss chromatograms (PMLCs; Figure 4). PMLCs correspond to the percent of signal lost from the weathered sample chromatogram relative to the original MW oil chromatogram, computed for each pixel (normalized to  $C_{30}$   $17\alpha(H),21\beta(H)$ -hopane). These operations were enabled by low retention time variability between chromatograms, further improved by chromatogram alignment. The root mean squared deviation (rmsd) values of the positions of the alignment points used were 0.9 and 5.4 pixels in first and second dimension, respectively, before alignment. After alignment, rmsd values were reduced to 0.5 and 2.4 pixels, according to the leave-one-out test described in Gros et al.,<sup>45</sup> indicating good retention time matching between chromatograms. On PMLCs, the position of the evaporation front, corresponding to a systematic removal of compounds along the first dimension,<sup>23</sup> can be identified easily (e.g., near  $n-C_{18}$  for sample B86; near  $n-C_{19}$  for sample B92). PMLCs allow comparisons within compound classes: on visual inspection, there appears to be no preferential degradation among different methylalkane isomers, and alkylcyclohexanes and alkylcyclopentanes also appear degraded to similar extents (Figure 4).

#### Percent Mass Losses of Saturates Compound Classes.

To quantify degradation extent for saturates eluting in the  $n-C_{17}$ – $n-C_{29}$  window, we computed peak volumes inside designated rectangular borders: rectangular boxes were drawn on the GC×GC chromatograms (Figure 3b), and the volumes of the resolved peaks situated within each box were estimated by the sum of the pixels contained in the box after applying Eilers' baseline correction (see "Data Analysis" in Methods).

Several distinct degradation patterns are visible (Figures 5 and SI S-8). Normal alkanes are initially preferentially lost (Figures 4, 5, and SI S-8), consistent with their known high susceptibility to biodegradation.<sup>3,16</sup> In the original MW oil,  $n$ -alkanes represent 40–50% of the total resolved mass of the saturates in the GC×GC subregion studied, but these compounds are  $>95\%$  depleted from the most weathered samples (Figure 5). Methylalkanes and alkylcyclopentanes+alkylcyclohexanes are degraded to similar extents throughout the sample set, independently of the position of the methyl group. They are degraded concomitantly with  $n$ -alkanes but to a lesser extent than  $n$ -alkanes. For all but the least weathered samples (B86 and B48,  $<20\%$   $n$ -alkanes depletion), acyclic and cyclic isoprenoid saturates exhibit the lowest extent of degradation compared to the other saturates classes. In the most weathered samples, the resolved signal in the subregion studied is dominated by isoprenoid saturates (27–33%; SI Figure S-8).

We think that biodegradation is the principal transformation process affecting  $>C_{22}$  saturates in the samples studied here, rather than photodegradation. The biodegradability of saturated hydrocarbons is widely established.<sup>3,4,16,32</sup> Indirect photodegradation of saturates has been observed in both laboratory and field studies.<sup>19,20</sup> However, compared to other petroleum hydrocarbons, saturates are the least susceptible to indirect photodegradation,<sup>7,53,56</sup> and the relevant time frames for photo-oxidation of saturates under environmental conditions are not

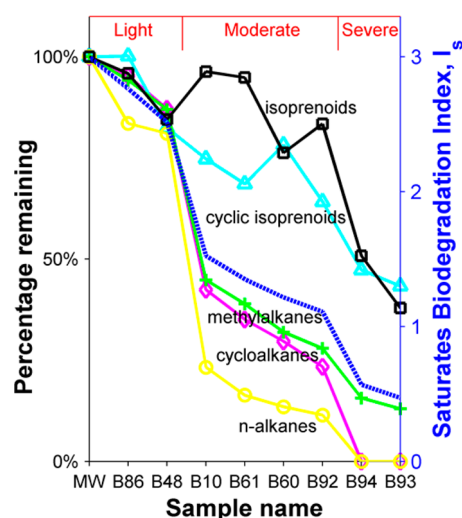


**Figure 5.** Percentage remaining for different classes of saturates eluting in the  $n-C_{22}$ – $n-C_{29}$  elution range, relative to the original MW oil, after normalization to  $C_{30}$   $17\alpha(H),21\beta(H)$ -hopane (left axis). Samples are ordered from least to most biodegraded (bottom axis). Saturates biodegradation index values as given by eq 1,  $I_s$  (blue dashed line), are shown for each sample (right axis), and corresponding biodegradation classifications (light, moderate, severe) are displayed (top axis).

well established. Among the five saturates families that we studied, extent of mass loss is found to decrease in the following order:  $n$ -alkanes  $>$  methylalkanes and alkylcyclopentanes+alkylcyclohexanes  $>$  cyclic and acyclic isoprenoids. This depletion pattern is consistent with previous findings that biodegradation rates of aliphatic compounds decrease progressively with increased branching of the molecular structure.<sup>3,32,57</sup> In contrast, we expect photogenerated oxidants to attack aliphatic compounds with rates decreasing in the following order: highly branched  $>$  less-branched  $>$  non-branched.<sup>58,59</sup> Hence, in our samples, the observed loss patterns for saturates are consistent with a biodegradation process, which is expected to transform less-branched saturates more quickly than more-branched saturates, whereas abiotic oxidation processes would be expected to produce the opposite mass loss pattern.

**New Biodegradation Index for Oil Weathering in Surface Environments.** Aware of the biases in traditional indices for biodegradation (see Introduction), we propose a new diagnostic for saturates biodegradation in moderately weathered oils in surface environments. We developed an index that incorporates information about the observed losses of the five different saturates classes considered here. The "saturates biodegradation index",  $I_s$ , was defined as:

$$I_s = F_n + F_b + F_i \quad (1)$$

where  $F_n$  is the fraction of  $n-C_{22}$ – $n-C_{29}$   $n$ -alkanes remaining in the weathered sample relative to original MW oil;  $F_b$  is the fraction remaining for alkylcyclopentanes+alkylcyclohexanes and methylalkanes in the  $n-C_{22}$ – $n-C_{29}$  elution window; and  $F_i$  is the fraction remaining for acyclic and cyclic isoprenoid compounds in this window. For the terms where two compound classes are grouped together (for example,  $F_i$  groups cyclic isoprenoids and acyclic isoprenoids), the term corresponds to the mean value of the two fractions remaining for the two classes. For each compound class, the fraction remaining is computed with respect to the original MW oil content

normalized to  $C_{30}$  17 $\alpha$ (H),21 $\beta$ (H)-hopane. The index definition is independent of the quantification procedure, and alternative quantification procedures could be used, assuming they are reliable for the compounds incorporated into eq 1. By excluding compounds eluting before  $n$ -C<sub>22</sub>, the index is designed to be unaffected by evaporation processes relevant to surface environments. The new biodegradation index may vary between a value of 3 (corresponding to the saturates composition of the original oil) and a value of 0 (corresponding to complete degradation of the five classes of saturates considered by the index). We defined index values of  $3 > I_s > 2$  as “light” biodegradation,  $2 > I_s > 1$  as “moderate” biodegradation, and  $1 > I_s > 0$  as “severe” biodegradation.

Ordering our samples by weathering extent according to  $I_s$  (Figure 5), we obtain a sequence similar to that inferred from  $n$ -C<sub>18</sub>/phytane ratios computed for the same samples by Aeppli et al.<sup>11</sup> In fact,  $I_s$  was found to correlate well with the  $n$ -C<sub>18</sub>/phytane ratio ( $r^2 = 0.95$ ; SI Figure S-10), for this sample set, corroborating previous evidence that the  $n$ -C<sub>18</sub>/phytane ratio is a good indicator of saturates biodegradation.<sup>3,16,30</sup> However, removal by evaporation appeared to be important for compounds eluting up to  $n$ -C<sub>18</sub> or  $n$ -C<sub>19</sub>, depending on the sample (Figure 4); consequently some evaporation impact on the  $n$ -C<sub>18</sub>/phytane ratio cannot be ruled out, since  $n$ -C<sub>18</sub> and phytane likely have slightly different vapor pressures. ( $n$ -C<sub>18</sub> and phytane exhibit slightly different GC×GC first dimension elution times, indicative of a difference in vapor pressures.<sup>52</sup>) We consider the new saturates index,  $I_s$ , to be more robust than previously proposed biodegradation indices for saturates. Equation 1 incorporates information about five major classes of saturates that span a broad range of susceptibility to biodegradation.

According to the new index, biodegradation extent is correlated to time of environmental exposure: ordering our samples by  $I_s$  value corresponds roughly to ordering them by sampling time (SI Figure S-9). Some discrepancies exist between samples taken at similar times, reflecting differences in the individual histories of the investigated sand patties. Three samples were taken in relatively dry beach locations, away from the shoreline (B86, B48, and B92), whereas the other samples were taken from within or near the surf zone and were considered as wet locations (SI Table S-1). The samples from dry locations all exhibit higher  $I_s$  values than samples collected from wet locations at the same period. Samples taken from wet locations exhibited low sample-to-sample variability at each sampling time point, and these samples display a consistent trend of decreasing  $I_s$  value with increasing time (SI Figure S-9). The quantitative differentiation of biodegradation extent in wet versus dry beach environments provides direct information about exposures faced by organisms in these different habitats. Additionally, the observed disparities in  $I_s$  values in wet environments versus dry environments support the interpretation that depletion of  $>C_{22}$  saturates resulted primarily from biodegradation rather than from indirect photodegradation.

**Implications for Oil Weathering in the Environment.** GC×GC elucidates compositional differences in UCMs that appear otherwise similar with conventional GC analysis. This allowed us to quantify differences in biodegradation extent among five classes of saturates in weathered oil samples taken from several field sites. For these compound classes, we find that biodegradation is not a simple stepwise process. Rather, different classes are consumed simultaneously but to different

extents, implying different biodegradation rates for these compounds. These results are based on the unprecedented quantification of relative abundances of several saturates classes achieved by the GC×GC techniques applied here. Our results are consistent with previous indications that increased aliphatic branching is associated with decreased biodegradation rate,<sup>57</sup> as well as previous evidence for the preferential biodegradation of  $n$ -alkanes versus isoprenoids.<sup>3</sup>

On the basis of the characteristic degradation patterns of saturates identified in weathered oil samples, we propose a new quantitative biodegradation index that allows the classification and ordering of samples having different biodegradation extent. The proposed biodegradation index succinctly and quantitatively conveys the time-dependent compositional evolution of  $>C_{22}$  saturates, analogous to the traditional  $n$ -C<sub>17</sub>/pristane and  $n$ -C<sub>18</sub>/phytane ratios.<sup>30,60–63</sup> Observed index variability among different samples is explained by residence time in the surface environment and by the suitability of local conditions for biodegradation. The index is a transferable metric to quantify these differences in biodegradation extent among different samples. The  $>C_{22}$  saturates represent a large fraction of the persistent oil residues. Thus the proposed index could inform overall mass balance estimates of weathered oil persisting from the *Deepwater Horizon* release, and it may also be a useful indicator in toxicity assessments of this long-lived material.

What did our samples reveal about the fate of MW oil in Gulf of Mexico coastal environments? Example mass apportionment calculations are shown here for our most weathered sample, B93, collected 19 months after the beginning of the oil release. Compounds lighter than  $n$ -C<sub>16</sub> were totally absent from sample B93, with partial mass losses observed in the  $n$ -C<sub>16</sub>– $n$ -C<sub>22</sub> elution region. For this sample, observed  $\leq n$ -C<sub>22</sub> losses correspond to 59% of the original MW oil mass (SI Figure S-10), based on GC×GC chromatogram data and simulated distillation data.<sup>41,64</sup> This loss pattern is consistent with removal by evaporation and dissolution, but photodegradation and biodegradation also probably participated in the mass depletion of the  $\leq n$ -C<sub>22</sub> fraction. In this same sample, mass losses in the  $>n$ -C<sub>22</sub> elution region correspond to a disappearance of 9% of the original oil mass, and this is attributed primarily to biodegradation (SI Figure S-11). Additionally, based on simulated distillation data, 14% of the original MW oil mass is not GC×GC-amenable and its fate cannot be assessed with this technique.<sup>41,64</sup> After accounting for these different apportionments for sample B93, 18% of the original MW oil mass was estimated to remain in the GC×GC chromatogram (SI Figure S-11). The original MW oil contained 8–10%  $>n$ -C<sub>22</sub> saturates (our estimate), and sample B93 still contained more than half (56%) of this original  $>n$ -C<sub>22</sub> saturates load. These example calculations are relevant to the 38–68 thousand metric tons of  $>C_{22}$  saturates material released into the marine environment during the *Deepwater Horizon* disaster.

Consideration of both GC-amenable and non-GC-amenable fractions of weathered sample B93 leads to a more global understanding of the fate of MW oil (Figure 6). According to silica-gel flash column chromatography analysis,  $2/3$  of sample B93 was constituted of mostly non-GC-amenable oxygenated compounds, and the bulk sample contained 9.8% oxygen (compared to the oxygen content of 0.4% in MW oil).<sup>11</sup> Hence 31% of the initial oil mass remained in the most weathered sample as oxygenated residues, invisible to GC-based analysis (SI Section S-10). Therefore disappearance of compounds from the GC×GC chromatogram should not be regarded as

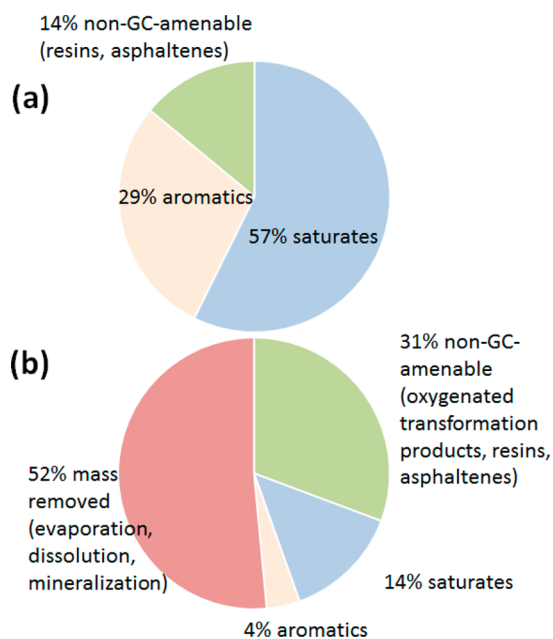


**Figure 6.** (a) Composition of the original MW oil, based on simulated distillation data (non-GC-amenable percentage)<sup>41,64</sup> and silica-gel flash column chromatography analysis.<sup>11</sup> (b) Apportionment of the oil that led to sample B93, including compounds removed through mass transfer or mineralization, and remaining mass, further divided into aromatics, saturates and oxygenated compounds based on silica-gel flash column chromatography data.<sup>11</sup>

synonymous with removal from the weathered sample, because a significant fraction of the weathered oil cannot be measured with this technique and may remain in the residue as transformation products. Formation of oxygenated products (carboxylic acids) during oil aerobic biodegradation has been previously reported.<sup>61</sup> Recent analysis shows that disappearance of some saturates correlates with the formation of (mostly non-GC-amenable) oxygenated weathering products.<sup>65</sup> Straight-chained carboxylic acids, attributed to degradation products of saturated hydrocarbons, were also recently identified in these samples.<sup>11</sup> Carboxylic acid-substituted degradation products of these saturated hydrocarbons may have direct environmental impact: terminal carboxylic acid derivatives of several saturates classes have been found toxic to aquatic organisms.<sup>66</sup>

In summary, in the warm climate of the Gulf of Mexico, which favors rapid weathering, mass transfer and mineralization processes are estimated to have removed only 52% of the original oil load from our most weathered oil-soaked sand patty (B93), 19 months after the explosion of the *Deepwater Horizon* platform (Figure 6b and SI Section S-10). The remaining 48% manifests as a mixture of persistent and partly degraded compounds, consisting of aromatics (4%), saturated hydrocarbons (14%), and non-GC-amenable oxygenated compounds (31%), in sample B93 (Figure 6b).

## ■ ASSOCIATED CONTENT

### ● Supporting Information

Detailed sample information; photographs and GC-FID chromatograms of selected samples; GC×GC-TOF-MS method; position of alignment points used; ions generated by the compounds studied; selected GC×GC-TOF-MS chromatograms; mass spectra of tridecylcyclohexane and 2-methylnonadecane; percentages of selected diagnostic ions in total mass

spectra of these two compounds; standards GC×GC-TOF-MS total ion current chromatogram displaying elution patterns of several saturates compounds; figure of percentages of the 5 saturates class studied in each sample; plot of sample  $I_s$  values versus sampling date; plot of  $I_s$  versus  $n\text{-C}_{18}$ /phytane ratio; and detailed calculation of the apportionment of the oil that led to B93. This information is available free of charge via the Internet at <http://pubs.acs.org>

## ■ AUTHOR INFORMATION

### Corresponding Author

\*Phone: +41 21 693 80 31; e-mail: [samuel.arey@epfl.ch](mailto:samuel.arey@epfl.ch).

### Present Address

<sup>||</sup>Bigelow Laboratory for Ocean Sciences, 60 Bigelow Drive, P.O. Box 380, East Boothbay, Maine 04544, United States.

### Author Contributions

The manuscript was written through contributions of all authors. All authors have given approval to the final version of the manuscript.

### Notes

The authors declare no competing financial interest.

## ■ ACKNOWLEDGMENTS

This research was supported by grants from the NSF (OCE-0960841 and EAR-0950600), the BP/the Gulf of Mexico Research Initiative (GoMRI-015), and the DEEP-C consortium. We thank Paul H. C. Eilers for allowing free access to his baseline correction code.

## ■ REFERENCES

- (1) Wolfe, D. A.; Hameedi, M. J.; Galt, J. A.; Watabayashi, G.; Short, J.; O'Claire, C.; Rice, S.; Michel, J.; Payne, J. R.; Braddock, J.; Hanna, S.; Sale, D. The fate of the oil spilled from the *Exxon Valdez*. *Environ. Sci. Technol.* **1994**, *28*, 560A–568A.
- (2) Wang, Z.; Fingas, M.; Blenkinsopp, S.; Sergy, G.; Landriault, M.; Sigouin, L.; Foght, J.; Semple, K.; Westlake, D. W. S. Comparison of oil composition changes due to biodegradation and physical weathering in different oils. *J. Chromatogr. A* **1998**, *809*, 89–107.
- (3) Prince, R. C.; Walters, C. C. Biodegradation of oil hydrocarbons and its implications for source identification. In *Oil Spill Environmental Forensics*; Wang, Z., Stout, S. A., Eds.; Academic Press: Burlington, MA, 2007; pp 349–379.
- (4) *Oil in the Sea III: Inputs, Fates, and Effects*; The National Academies Press: Washington, DC, 2003.
- (5) Irvine, G. V.; Mann, D. H.; Short, J. W. Persistence of 10-year old *Exxon Valdez* oil on Gulf of Alaska beaches: The importance of boulder-armoring. *Mar. Pollut. Bull.* **2006**, *52*, 1011–1022.
- (6) Wardlaw, G. D.; Arey, J. S.; Reddy, C. M.; Nelson, R. K.; Ventura, G. T.; Valentine, D. L. Disentangling oil weathering at a marine seep using GC×GC: Broad metabolic specificity accompanies subsurface petroleum biodegradation. *Environ. Sci. Technol.* **2008**, *42*, 7166–7173.
- (7) Prince, R. C.; Garrett, R. M.; Bare, R. E.; Grossman, M. J.; Townsend, T.; Suflita, J. M.; Lee, K.; Owens, E. H.; Sergy, G. A.; Braddock, J. F.; Lindstrom, J. E.; Lessard, R. R. The roles of photooxidation and biodegradation in long-term weathering of crude and heavy fuel oils. *Spill Sci. Technol. Bull.* **2003**, *8*, 145–156.
- (8) Sextstone, A.; Gustin, P.; Atlas, R. M. Long term interactions of microorganisms and Prudhoe Bay crude oil in tundra soils at Barrow, Alaska. *ARCTIC* **1978**, *31*, 348–354.
- (9) Scarlett, A. G. Effect-directed analysis of toxicants in unresolved complex mixtures (UCMs) of hydrocarbons from biodegraded crude oils. Ph.D. Dissertation, University of Plymouth, Plymouth, MA, 2007.
- (10) Brownawell, B. J.; Dick, J.; McElroy, A. E.; Reddy, C. M.; Nelson, R. K. *The Environmental Implications of the UCM in Sediments of the New York Harbor Complex*; A final report to the Hudson River

Foundation on contract 002/003A; Stony Brook University: Stony Brook, NY, 2007.

(11) Aeppli, C.; Carmichael, C. A.; Nelson, R. K.; Lemkau, K. L.; Graham, W. M.; Redmond, M. C.; Valentine, D. L.; Reddy, C. M. Oil weathering after the *Deepwater Horizon* disaster led to the formation of oxygenated residues. *Environ. Sci. Technol.* **2012**, *46*, 8799–8807.

(12) Gough, M. A.; Rowland, S. J. Characterization of unresolved complex mixtures of hydrocarbons in petroleum. *Nature* **1990**, *344*, 648–650.

(13) Stout, S. A.; Wang, Z. Chemical fingerprinting of spilled or discharged petroleum: methods and factors affecting petroleum fingerprints in the environment. In *Oil Spill Environmental Forensics*; Wang, Z., Stout, S. A., Eds.; Academic Press: Burlington, MC, 2007; pp 1–53.

(14) Arey, J. S.; Nelson, R. K.; Plata, D. L.; Reddy, C. M. Disentangling oil weathering using GC×GC. 2. Mass transfer calculations. *Environ. Sci. Technol.* **2007**, *41*, 5747–5755.

(15) Reddy, C. M.; Eglinton, T. I.; Hounshell, A.; White, H. K.; Xu, L.; Gaines, R. B.; Frysinger, G. S. The West Falmouth oil spill after thirty years: The persistence of petroleum hydrocarbons in marsh sediments. *Environ. Sci. Technol.* **2002**, *36*, 4754–4760.

(16) Peters, K. E.; Walters, C. C.; Moldowan, J. M. *The Biomarker Guide, Biomarkers and Isotopes in Petroleum Exploration and Earth History*; 2nd ed.; Cambridge University Press: Cambridge, 2005; Vol. 2.

(17) Prince, R. C.; Elmendorf, D. L.; Lute, J. R.; Hsu, C. S.; Haith, C. E.; Senius, J. D.; Dechert, G. J.; Douglas, G. S.; Butler, E. L. 17 $\alpha$ (H)-21 $\beta$ (H)-hopane as a conserved internal marker for estimating the biodegradation of crude oil. *Environ. Sci. Technol.* **1994**, *28*, 142–145.

(18) Wang, Z.; Fingas, M.; Owens, E. H.; Sigouin, L.; Brown, C. E. Long-term fate and persistence of the spilled *Metula* oil in a marine salt marsh environment: Degradation of petroleum biomarkers. *J. Chromatogr. A* **2001**, *926*, 275–290.

(19) Charrié-Duhaut, A.; Lemoine, S.; Adam, P.; Connan, J.; Albrecht, P. Abiotic oxidation of petroleum bitumens under natural conditions. *Org. Geochem.* **2000**, *31*, 977–1003.

(20) Guiliano, M.; El Anba-Lurot, F.; Doumenq, P.; Mille, G.; Rontani, J. F. Photo-oxidation of *n*-alkanes in simulated marine environmental conditions. *J. Photochem. Photobiol. Chem.* **1997**, *102*, 127–132.

(21) Gesser, H. D.; Wildman, T. A.; Tewari, Y. B. Photooxidation of *n*-hexadecane sensitized by xanthone. *Environ. Sci. Technol.* **1977**, *11*, 605–608.

(22) Wang, Z.; Fingas, M.; Sergy, G. Chemical characterization of crude oil residues from an Arctic beach by GC/MS and GC/FID. *Environ. Sci. Technol.* **1995**, *29*, 2622–2631.

(23) Arey, J. S.; Nelson, R. K.; Reddy, C. M. Disentangling oil weathering using GC×GC. 1. Chromatogram analysis. *Environ. Sci. Technol.* **2007**, *41*, 5738–5746.

(24) Ventura, G. T.; Kenig, F.; Reddy, C. M.; Frysinger, G. S.; Nelson, R. K.; Mooy, B. V.; Gaines, R. B. Analysis of unresolved complex mixtures of hydrocarbons extracted from Late Archean sediments by comprehensive two-dimensional gas chromatography (GC×GC). *Org. Geochem.* **2008**, *39*, 846–867.

(25) Tran, T. C.; Logan, G. A.; Grosjean, E.; Ryan, D.; Marriott, P. J. Use of comprehensive two-dimensional gas chromatography/time-of-flight mass spectrometry for the characterization of biodegradation and unresolved complex mixtures in petroleum. *Geochim. Cosmochim. Acta* **2010**, *74*, 6468–6484.

(26) Garrett, R. M.; Rothenburger, S. J.; Prince, R. C. Biodegradation of fuel oil under laboratory and arctic marine conditions. *Spill Sci. Technol. Bull.* **2003**, *8*, 297–302.

(27) Olson, J. J.; Mills, G. L.; Herbert, B. E.; Morris, P. J. Biodegradation rates of separated diesel components. *Environ. Toxicol. Chem.* **1999**, *18*, 2448–2453.

(28) Mao, D.; Lookman, R.; Weghe, H. V. D.; Weltens, R.; Vanermen, G.; Brucker, N. D.; Diels, L. Combining HPLC-GC×GC, GC×GC/ToF-MS, and selected ecotoxicity assays for detailed

monitoring of petroleum hydrocarbon degradation in soil and leaching water. *Environ. Sci. Technol.* **2009**, *43*, 7651–7657.

(29) Miralles, G.; Grossi, V.; Acquaviva, M.; Duran, R.; Bertrand, J. C.; Cuny, P. Alkane biodegradation and dynamics of phylogenetic subgroups of sulfate-reducing bacteria in an anoxic coastal marine sediment artificially contaminated with oil. *Chemosphere* **2007**, *68*, 1327–1334.

(30) Blumer, M.; Sass, J. Oil pollution: Persistence and degradation of spilled fuel oil. *Science* **1972**, *176*, 1120–1122.

(31) Wenger, L. M.; Davis, C. L.; Isaksen, G. H. Multiple controls on petroleum biodegradation and impact on oil quality. *SPE Reservoir Eval. Eng.* **2002**, 375–383.

(32) Wardroper, A. M. K.; Hoffmann, C. F.; Maxwell, J. R.; Barwise, A. J. G.; Goodwin, N. S.; Park, P. J. D. Crude oil biodegradation under simulated and natural conditions. II. Aromatic steroid hydrocarbons. *Org. Geochem.* **1984**, *6*, 605–617.

(33) Rowland, S.; Donkin, P.; Smith, E.; Wraige, E. Aromatic hydrocarbon “humps” in the marine environment: Unrecognized toxins? *Environ. Sci. Technol.* **2001**, *35*, 2640–2644.

(34) Neff, J. M.; Ostazeski, S.; Gardiner, W.; Stejskal, I. Effects of weathering on the toxicity of three offshore Australian crude oils and a diesel fuel to marine animals. *Environ. Toxicol. Chem.* **2000**, *19*, 1809–1821.

(35) Scarlett, A.; Galloway, T. S.; Rowland, S. J. Chronic toxicity of unresolved complex mixtures (UCM) of hydrocarbons in marine sediments. *J. Soils Sed.* **2007**, *7*, 200–206.

(36) Nelson, R. K.; Kile, B. M.; Plata, D. L.; Sylva, S. P.; Xu, L.; Reddy, C. M.; Gaines, R. B.; Frysinger, G. S.; Reichenbach, S. E. Tracking the weathering of an oil spill with comprehensive two-dimensional gas chromatography. *Environ. Forensics* **2006**, *7*, 33–44.

(37) Frysinger, G. S.; Gaines, R. B.; Xu, L.; Reddy, C. M. Resolving the unresolved complex mixture in petroleum-contaminated sediments. *Environ. Sci. Technol.* **2003**, *37*, 1653–1662.

(38) Gaines, R. B.; Frysinger, G. S.; Reddy, C. M.; Nelson, R. K. Oil spill source identification by comprehensive two-dimensional gas chromatography (GC×GC). In *Oil Spill Environmental Forensics*; Wang, Z., Stout, S. A., Eds.; Academic Press: Burlington, MA, 2007; pp 169–206.

(39) Mao, D.; Lookman, R.; Van De Weghe, H.; Van Look, D.; Vanermen, G.; De Brucker, N.; Diels, L. Detailed analysis of petroleum hydrocarbon attenuation in biopiles by high-performance liquid chromatography followed by comprehensive two-dimensional gas chromatography. *J. Chromatogr. A* **2009**, *1216*, 1524–1527.

(40) Atlas, R. M.; Hazen, T. C. Oil biodegradation and bioremediation: A tale of the two worst spills in U.S. history. *Environ. Sci. Technol.* **2011**, *45*, 6709–6715.

(41) Reddy, C. M.; Arey, J. S.; Seewald, J. S.; Sylva, S. P.; Lemkau, K. L.; Nelson, R. K.; Carmichael, C. A.; McIntyre, C. P.; Fenwick, J.; Ventura, G. T.; Mooy, B. A. S. V.; Camilli, R. Composition and fate of gas and oil released to the water column during the *Deepwater Horizon* oil spill. *Proc. Natl. Acad. Sci., U. S. A.* **2012**, *109*, 20229–20234.

(42) McNutt, M. K.; Camilli, R.; Crone, T. J.; Guthrie, G. D.; Hsieh, P. A.; Ryerson, T. B.; Savas, O.; Shaffer, F. Review of flow rate estimates of the *Deepwater Horizon* oil spill. *Proc. Natl. Acad. Sci., U. S. A.* **2012**, *109*, 20260–20267.

(43) Reichenbach, S. E.; Ni, M.; Zhang, D.; Ledford, E. B., Jr. Image background removal in comprehensive two-dimensional gas chromatography. *J. Chromatogr. A* **2003**, *985*, 47–56.

(44) Eilers, P. H. C. Parametric time warping. *Anal. Chem.* **2004**, *76*, 404–411.

(45) Gros, J.; Nabi, D.; Dimitriou-Christidis, P.; Rutler, R.; Arey, J. S. Robust algorithm for aligning two-dimensional chromatograms. *Anal. Chem.* **2012**, *84*, 9033–9040.

(46) Reichenbach, S. E.; Ni, M.; Kottapalli, V.; Visvanathan, A. Information technologies for comprehensive two-dimensional gas chromatography. *Chemom. Intell. Lab. Syst.* **2004**, *71*, 107–120.

(47) *ChromaTOF Software Instruction Manual, Version 4.2x*; Leco Corporation: St. Joseph, MO, 2009.

(48) Mao, D.; Lookman, R.; Van De Weghe, H.; Vanermen, G.; De Brucker, N.; Diels, L. Aqueous solubility calculation for petroleum mixtures in soil using comprehensive two-dimensional gas chromatography analysis data. *J. Chromatogr. A* **2009**, *1216*, 2873–2880.

(49) Fryzinger, G. S.; Gaines, R. B.; Ledford, E. B., Jr. Quantitative determination of BTEX and total aromatic compounds in gasoline by comprehensive two-dimensional gas chromatography (GC×GC). *J. High Resolut. Chromatogr.* **1999**, *22*, 195–200.

(50) Farrington, J. W.; Teal, J. M.; Quinn, J. G.; Wade, T.; Burns, K. Intercalibration of analyses of recently biosynthesized hydrocarbons and petroleum hydrocarbons in marine lipids. *Bull. Environ. Contam. Toxicol.* **1973**, *10*, 129–136.

(51) Sutton, P. A.; Lewis, C. A.; Rowland, S. J. Isolation of individual hydrocarbons from the unresolved complex hydrocarbon mixture of a biodegraded crude oil using preparative capillary gas chromatography. *Org. Geochem.* **2005**, *36*, 963–970.

(52) Arey, J. S.; Nelson, R. K.; Xu, L.; Reddy, C. M. Using comprehensive two-dimensional gas chromatography retention indices to estimate environmental partitioning properties for a complete set of diesel fuel hydrocarbons. *Anal. Chem.* **2005**, *77*, 7172–7182.

(53) Schwarzenbach, R. P.; Gschwend, P. M.; Imboden, D. M. *Environmental Organic Chemistry*; John Wiley & Sons, Inc.: Hoboken, NJ, 2005.

(54) Ezra, S.; Feinstein, S.; Pelly, I.; Bauman, D.; Miloslavsky, I. Weathering of fuel oil spill on the east Mediterranean coast, Ashdod, Israel. *Org. Geochem.* **2000**, *31*, 1733–1741.

(55) Douglas, G. S.; Owens, E. H.; Hardenstine, J.; Prince, R. C. The OSSA II pipeline oil spill: The character and weathering of the spilled oil. *Spill Sci. Technol. Bull.* **2002**, *7*, 135–148.

(56) King, S. M.; Leaf, P. A.; Olson, A. C.; Ray, P. Z.; Tarr, M. A. Photolytic and photocatalytic degradation of surface oil from the Deepwater Horizon spill. *Chemosphere* **2014**, *95*, 415–422.

(57) Howard, P. H. Biodegradation. In *Handbook of Property Estimation Methods for Chemicals: Environmental and Health Sciences*; CRC Press: Boca Raton, FL, 2000; p 467.

(58) Kwok, E.; Atkinson, R. Estimation of hydroxyl radical reaction rate constants for gas-phase organic compounds using a structure-reactivity relationship - An update. *Atmos. Environ.* **1995**, *29*, 1685–1695.

(59) Neeb, P. Structure-reactivity based estimation of the rate constants for hydroxyl radical reactions with hydrocarbons. *J. Atmos. Chem.* **2000**, *35*, 295–315.

(60) Elordui-Zapatarietxe, S.; Rosell-Melé, A.; Moraleda, N.; Tolosa, I.; Albaigés, J. Phase distribution of hydrocarbons in the water column after a pelagic deep ocean oil spill. *Mar. Pollut. Bull.* **2010**, *60*, 1667–1673.

(61) Watson, J. S.; Jones, D. M.; Swannell, R. P. J.; van Duin, A. C. T. Formation of carboxylic acids during aerobic biodegradation of crude oil and evidence of microbial oxidation of hopanes. *Org. Geochem.* **2002**, *33*, 1153–1169.

(62) Wang, Z.; Fingas, M. Differentiation of the source of spilled oil and monitoring of the oil weathering process using gas chromatography-mass spectrometry. *J. Chromatogr. A* **1995**, *712*, 321–343.

(63) Lemkau, K. L.; Peacock, E. E.; Nelson, R. K.; Ventura, G. T.; Kovacs, J. L.; Reddy, C. M. The M/V Cosco Busan spill: Source identification and short-term fate. *Mar. Pollut. Bull.* **2010**, *60*, 2123–2129.

(64) Carmichael, C. A.; Arey, J. S.; Graham, W. M.; Linn, L. J.; Lemkau, K. L.; Nelson, R. K.; Reddy, C. M. Floating oil-covered debris from Deepwater Horizon: Identification and application. *Environ. Res. Lett.* **2012**, *7*, 015301.

(65) Hall, G. J.; Fryzinger, G. S.; Aeppli, C.; Carmichael, C. A.; Gros, J.; Lemkau, K. L.; Nelson, R. K.; Reddy, C. M. Oxygenated weathering products of Deepwater Horizon oil come from surprising precursors. *Mar. Pollut. Bull.* **2013**, *75*, 140–149.

(66) Jones, D.; Scarlett, A. G.; West, C. E.; Rowland, S. J. Toxicity of individual naphthenic acids to *Vibrio fischeri*. *Environ. Sci. Technol.* **2011**, *45*, 9776–9782.